Physics Letters B 728 (2014) 450–456

Contents lists available at ScienceDirect

Physics Letters B

www.elsevier.com/locate/physletb

The charged Lifshitz black brane geometry and the bulk dipole coupling

Jian-Pin Wu

Department of Physics, School of Mathematics and Physics, Bohai University, JinZhou, 121013, China

ARTICLE INFO

Article history:
Received 30 August 2013
Received in revised form 9 November 2013
Accepted 19 November 2013
Available online 22 November 2013
Editor: M. Cvetič

ABSTRACT

We study the fermionic response including the bulk dipole coupling on the charged Lifshitz black brane from Einstein–Dilaton–Maxwell model. For fixed Lifshitz dynamical critical exponent z, by tuning the dipole coupling parameter p, we can realize the phase transitions from Fermi liquid, to marginal Fermi liquid, to non-Fermi liquid and finally to Mott insulator. The Lifshitz dynamical critical exponent z plays the role of making the phase transition point from Fermi liquid to non-Fermi liquid or to Mott insulator decrease with the increase of z for fixed dipole coupling p.

1. Introduction

The AdS/CFT correspondence [1–3] has been widely recognized as a powerful tool to offer insight into the dynamics of strongly coupled quantum field theories. Recently, the AdS/CFT correspondence has also been applied in condensed matter theory, which is called AdS/CMT correspondence, to understand some exotic but important numerous correlated electron materials, including the high temperature superconductor and the heavy fermion systems. By adding a probe free fermion on some gravity backgrounds, a Fermi surface usually emerges, which can exhibit Fermi liquid, marginal Fermi liquid, or non-Fermi liquid behaviors, depending on the mass and charge of the bulk fermion, or the other parameters of the specific gravity model (see for example [4–14]). On the other hand, if a coupling between the fermion and gauge field is introduced in some bulk geometries, which we call dipole coupling, we can observe that the dual field theory can model the Mott physics (see [15–24]).

In the above studies, they only focus on the case that the time and space is isotropic. However, as is known to all, in many condensed matter systems, the fixed point is usually described by the Lifshitz dynamical scaling $t \to \lambda^z t$, $\vec{x} \to \lambda \vec{x}$. The case of $z = 1$ corresponds to the relativistic fixed point, in which the time and space is isotropic. For $z > 1$, the isotropic between the time and space is broken, which we call the non-relativistic fixed point.

To achieve the Lifshitz fixed point in the dual field theory by AdS/CFT correspondence, the gravity description of Lifshitz fixed points is needed [25–38]. Usually, there are two ways to achieve the Lifshitz black hole geometry. One is to add a massive vector (Poca) field into the Einstein–Maxwell gravity system, which we refer to Einstein–Maxwell–Proca model (EMP model). The Proca field is an auxiliary field, which plays the role in modifying the asymptotic geometry from AdS to Lifshitz. For EMP model, only have some numerical solutions been found for generic Lifshitz exponent z [37] except the special case $z = 2(d-1)$ [31], where d is the dimension of the dual field theory. Another way is to introduce the dilaton field and a pair of $U(1)$ gauge fields and we refer this model as Einstein–Dilaton–Maxwell model (EDM model), which has an analytical black hole solution for generic Lifshitz exponent z [37,38].

Some pioneer works have been done to study the fermionic response on the Lifshitz geometry [39–43]. In Ref. [39], the retarded Green's function on Lifshitz background in the absence of the chemical potential has firstly been studied. Also, the non-relativistic fermionic retarded Green's function on Lifshitz geometry with critical exponent $z = 2$ [40] was worked out, where the chemical potential is also absent. They observe that a flat band emerges, similar with that on RN-AdS background [44]. On the other hand, the relativistic fermionic correlation function on a charged Lifshitz geometry (EMP model) for the special critical exponent $z = 2(d-1)$ has been studied in [41]. For $z = 2$, a linear dispersion relation is observed, but for $z = 4$ and $z = 6$, the Fermi sea vanishes. Subsequently, the dipole coupling effects on the Lifshitz geometry from EMP model are explored in [43]. However, due to the exact analytical solution for $z = 2(d-1)$ being only valid for finite temperature, we can only study the fermionic response at finite temperature. In order to explore the fermionic response on the extremal Lifshitz geometry, which can compare with that in extremal RN-AdS background [5,7], and to see how the fermionic

E-mail address: wujianpin@gmail.com.

0370-2693
http://dx.doi.org/10.1016/j.physletb.2013.11.040

response is controlled by the anisotropic scaling, the author in Ref. [37] study the properties of the fermionic Green's function on the Lifshitz geometry from EDM model [37].[1] They find that the dispersion relation on this background also depends on the Lifshitz dynamical exponent z. Especially, the Lifshitz dynamical exponent z plays the role smoothing out the quasi-particle-peak.

In this Letter, we will turn to explore the dipole coupling effects on this background. The rest parts of this Letter is organized as follows. In Section 2, a brief review on the charged Lifshitz black hole geometry from EDM theory will be given and the bulk Dirac equations, including dipole coupling term, on this background are derived. In Section 3, we will study the Fermi surface structure on this Lifshitz background for negative and small positive p. For the case of large positive p, we will present in Section 4. Finally, some concluding remarks are summarized in Section 5.

2. The charged Lifshitz black brane geometry and the bulk dipole coupling

In order to study the dipole coupling effects on the charged black brane geometry with Lifshitz dynamical critical exponent z, we consider the following action

$$S_{EDM}=\frac{1}{16\pi G_{d+1}}\int d^{d+1}x\sqrt{-g}\Big[R-2\Lambda-\frac{1}{2}\partial_a\phi\partial^a\phi-\frac{1}{4}\sum_{i=1}^{n}e^{\lambda_i\phi}F^{(i)ab}F^{(i)}_{ab}\Big]. \tag{1}$$

This action contains a dilaton field and a pair of $U(1)$ gauge fields, which we refer to Einstein–Dilaton–Maxwell action [37,38]. But here we will only consider the case of two $U(1)$ gauge fields $F^{(1)}_{rt}$ and $F^{(2)}_{rt}$, in which the first gauge field $F^{(1)}_{rt}$ plays the role of an auxiliary field and the second $F^{(2)}_{rt}$ is the real Maxwell field. This model admits the following black brane solution

$$ds^2=-\frac{r^{2z}}{L^{2z}}f(r)\,dt^2+\frac{L^2}{r^2}\frac{dr^2}{f(r)}+\frac{r^2}{L^2}d\vec{x}^2_{d-1}, \tag{2}$$

$$f(r)=1-\frac{M}{r^{d+z-1}}+\frac{Q^2}{r^{2(d+z-2)}}, \tag{3}$$

$$A^{(1)}_t=-\left(\frac{r_0}{L}\right)^z\sqrt{\frac{2(z-1)}{d+z-1}}\left[1-\left(\frac{r}{r_0}\right)^{d+z-1}\right], \tag{4}$$

$$A^{(2)}_t=\mu\left[1-\left(\frac{r_0}{r}\right)^{d+z-3}\right], \tag{5}$$

$$e^{\phi}=\left(\frac{r}{r_0}\right)^{\sqrt{2(d-1)(z-1)}}, \tag{6}$$

$$\Lambda=-\frac{(d+z-1)(d+z-2)}{2L^2}, \tag{7}$$

where we have defined

$$\mu\equiv\sqrt{\frac{2(d-1)}{d+z-3}}\frac{Q}{L^{z+1}r_0^{d-2}}. \tag{8}$$

Note that there are the following relations between the coupling constant λ_i in the action (1) and the Lifshitz dynamical exponent z

$$\lambda_1=-\sqrt{2\frac{d-1}{z-1}},\qquad \lambda_2=\sqrt{2\frac{z-1}{d-1}}. \tag{9}$$

[1] A minimally coupled charged scalar field in this Lifshitz background is studied in [46].

For the detailed discussions, we can refer to Refs. [37,38]. Different from the analytical black hole solution obtained in Ref. [31], which is valid only for $z=2(d-1)$ and finite temperature, this solution from EDM model is valid for generic dynamical exponent z at zero or finite temperature, which can provide us a Lifshitz geometry, on which we can study how the Lifshitz dynamical critical exponent z controls the holographic response system at zero and finite temperature. In addition, we also note that from Eq. (4), the auxiliary gauge field $A^{(1)}_t$ vanishes in the $z\to 1$ limit, which recovers to the case of RN-AdS black brane. For calculational purpose, we can make a rescaling so that we can set $L=1$ and $r_0=1$ [42], at which the metric (2) becomes

$$ds^2=-r^{2z}f(r)\,dt^2+\frac{1}{r^2f(r)}dr^2+r^2\,d\vec{x}^2_{d-1}, \tag{10}$$

with the redshift factor $f(r)$ and the gauge field $A^{(2)}_t$ being, respectively

$$f(r)=1-\frac{1+Q^2}{r^{d+z-1}}+\frac{Q^2}{r^{2(d+z-2)}}, \tag{11}$$

$$A^{(2)}_t=\mu\left[1-\left(\frac{1}{r}\right)^{d+z-3}\right]. \tag{12}$$

Also, we have the following dimensionless temperature

$$T=\frac{1}{4\pi}\left[d-1+z-\frac{(d-3+z)^2\mu^2}{2(d-1)}\right]. \tag{13}$$

The zero temperature limit can be obtained by setting $\mu=\frac{\sqrt{2(d-1)(d-1+z)}}{d-3+z}$, in which the redshift factor $f(r)$ becomes

$$f(r)|_{T=0}=1-2\frac{d+z-2}{d+z-3}\frac{1}{r^{d+z-1}}+\frac{d+z-1}{d+z-3}\frac{1}{r^{2(d+z-2)}}. \tag{14}$$

Near the horizon ($r\to 1$), we can easily find

$$f(r)|_{T=0,r\to 1}\simeq(d+z-1)(d+z-2)(r-1)^2\equiv\frac{1}{L_2^2}(r-1)^2, \tag{15}$$

where we have denoted $L_2\equiv 1/\sqrt{(d+z-1)(d+z-2)}$. Obviously, similar with that of RN-AdS black brane, the near horizon geometry at the zero temperature is also $AdS_2\times\mathbb{R}^{d-1}$ for this Lifshitz black brane from EDM model. But we note that L_2 of the curvature radius of AdS_2 is related to the dynamical exponent z. In this Letter, we will only focus on the extremal case.

Now we wish to take the dipole coupling effects into consideration. For this purpose, we consider the following action with the dipole interaction between the fermion and the gauge field [15–18]

$$S_D=i\int d^{d+1}x\sqrt{-g}\bar{\zeta}\big(\Gamma^a\mathcal{D}_a-m-ip\not{F}\big)\zeta, \tag{16}$$

where $\mathcal{D}_a=\partial_a+\frac{1}{4}(\omega_{\mu\nu})_a\Gamma^{\mu\nu}-iqA^{(2)}_a$ is the covariant derivative and $\not{F}=\frac{1}{4}\Gamma^{\mu\nu}(e_\mu)^a(e_\nu)^bF^{(2)}_{ab}$. A redefinition of $\zeta=(-gg^{rr})^{-\frac{1}{4}}\mathcal{F}$ can cancel off the spin connection contributions. At the same time, we will expand $\mathcal{F}$ as $\mathcal{F}=Fe^{-i\omega t+ik_ix^i}$ in the Fourier space. Thus the Dirac equation can be derived from the action (16)

$$\Big(\sqrt{g^{rr}}\Gamma^r\partial_r-m-\frac{ip}{2}\sqrt{g^{rr}g^{tt}}\Gamma^{rt}\partial_rA^{(2)}_t\Big)F-i\big(\omega+qA^{(2)}_t\big)\sqrt{g^{tt}}\Gamma^tF+ik\sqrt{g^{xx}}\Gamma^xF=0. \tag{17}$$

We have set $k_1 = k$ and $k_i \neq 0$, $i \neq 1$ without loss of generality. To solve the Dirac equation we choose the following basis for our gamma matrices[2]

$$\Gamma^r = \begin{pmatrix} -\sigma^3 & 0 \\ 0 & -\sigma^3 \end{pmatrix}, \qquad \Gamma^t = \begin{pmatrix} i\sigma^1 & 0 \\ 0 & i\sigma^1 \end{pmatrix},$$
$$\Gamma^x = \begin{pmatrix} -\sigma^2 & 0 \\ 0 & \sigma^2 \end{pmatrix}, \quad \ldots. \tag{18}$$

Then the Dirac equation reduces to

$$\Big[\big(\partial_r + m\sqrt{g_{rr}}\sigma^3\big) - \sqrt{\frac{g_{rr}}{g_{tt}}}\big(\omega + qA_t^{(2)}\big)i\sigma^2 - (-1)^I k\sqrt{\frac{g_{rr}}{g_{xx}}}\sigma^1 + p\sqrt{g^{tt}}\partial_r A_t^{(2)}\sigma^1\Big]F_I = 0, \tag{19}$$

where $I = 1, 2$. Furthermore we can explicitly split F_I into $F_I = (\mathcal{A}_I, \mathcal{B}_I)^T$ and so we have

$$(\partial_r + m\sqrt{g_{rr}})\mathcal{A}_I - \sqrt{\frac{g_{rr}}{g_{tt}}}\big(\omega + qA_t^{(2)}\big)\mathcal{B}_I - (-1)^I\sqrt{\frac{g_{rr}}{g_{xx}}}k\mathcal{B}_I = 0, \tag{20}$$

$$(\partial_r + m\sqrt{g_{rr}})\mathcal{B}_I + \sqrt{\frac{g_{rr}}{g_{tt}}}\big(\omega + qA_t^{(2)}\big)\mathcal{A}_I - (-1)^I\sqrt{\frac{g_{rr}}{g_{xx}}}k\mathcal{A}_I = 0. \tag{21}$$

It is convenient to package the above equations into a flow equation of ξ_I

$$(\partial_r + 2m\sqrt{g_{rr}})\xi_I - \Big[v_- + (-1)^I k\sqrt{\frac{g_{rr}}{g_{xx}}}\Big] - \Big[v_+ - (-1)^I k\sqrt{\frac{g_{rr}}{g_{xx}}}\Big]\xi_I^2 = 0, \tag{22}$$

where we have defined $\xi_I \equiv \frac{\mathcal{A}_I}{\mathcal{B}_I}$ and $v_\pm = \sqrt{\frac{g_{rr}}{g_{tt}}}(\omega + qA_t^{(2)}) \pm p\sqrt{g^{tt}}\partial_r A_t^{(2)}$.

Now, we will discuss how to read off the boundary Green's functions when the geometry near the boundary is asymptotic Lifshitz. By substituting the charged Lifshitz black brane geometry (10) into Eq. (19), one has

$$\Big(\partial_r + \frac{m}{r\sqrt{f}}\sigma^3\Big)F_I - \frac{1}{r^{z+1}f}\Big[\omega + q\Big(1 - \Big(\frac{1}{r}\Big)^z\Big)\Big]i\sigma^2 F_I - (-1)^I\frac{k}{r^2\sqrt{f}}\sigma^1 F_I + \frac{p\mu z}{r^{2z+1}\sqrt{f}}\sigma^1 F_I = 0. \tag{23}$$

Obviously, when $r \to \infty$, the above equation has the same form as the case of RN-AdS background

$$\big(r\partial_r + m\sigma^3\big)F_I \approx 0. \tag{24}$$

Therefore, even if the asymptotic geometry is Lifshitz, the asymptotic behavior for F_I has the same form as the AdS case

$$F_I \overset{r\to\infty}{\approx} a_I r^m \begin{pmatrix} 0 \\ 1 \end{pmatrix} + b_I r^{-m}\begin{pmatrix} 1 \\ 0 \end{pmatrix}. \tag{25}$$

Following the prescriptions of Ref. [45], if $a_I\begin{pmatrix} 0 \\ 1 \end{pmatrix}$ and $b_I\begin{pmatrix} 1 \\ 0 \end{pmatrix}$ are related by

$$b_I\begin{pmatrix} 1 \\ 0 \end{pmatrix} = \mathcal{S}a_I\begin{pmatrix} 0 \\ 1 \end{pmatrix}, \tag{26}$$

then the boundary Green's function G is given by

$$G = -i\mathcal{S}\gamma^0, \tag{27}$$

where $\gamma^0 = i\sigma^1$ is the gamma matrices of the boundary theory. So, by using Eqs. (25), (26) and (27), the boundary Green's function can be expressed as

$$G(\omega, k) = \lim_{r\to\infty} r^{2m}\begin{pmatrix} \xi_1 & 0 \\ 0 & \xi_2 \end{pmatrix}. \tag{28}$$

Again, we see that the expression of the fermionic Green's function on the Lifshitz boundary is same as that on the AdS boundary. In addition, to solve the flow Eq. (22) we need to impose the following in-falling boundary conditions at the horizon $r = 1$

$$\xi_I = i. \tag{29}$$

Before proceeding, we would like to point out that in the action (1) we have set the gauge coupling constant $g_F = 2$. It is different from the conventions of Refs. [15,16] where $g_F = 1$. Since the relevant quantities are the products $g_F q$ and $g_F p$, the charge q and the bulk dipole coupling p in our Letter will correspond to $q/2$ and $p/2$ in Refs. [15,16]. In addition, in Refs. [15,16], they make a rescaling $p \to pL/(d-2)$, but we don't here. In what follows, we will mostly work with the case of $m = 0$ and $q = 0.5$ without loss of generality.

3. The Fermi surface structure

In Ref. [42], we study how the Lifshitz dynamical critical exponent z affects the Fermi surface structure. Here, we will study how the Lifshitz dynamical critical exponent z and the bulk dipole coupling p affect together the Fermi surface structure.

As pointed out that in the above section, the extremal near horizon geometry is $AdS_2 \times \mathbb{R}^{d-1}$ so that we can determine the spectral function using the matching method [7]. For this purpose, near the horizon (near region) we make a coordinate change $\varsigma = \omega\frac{L_2^2}{r-1}$, $\tau = \omega t$ in the limit of $\omega \to 0$ so that the Dirac equation (19) can be written as

$$\varsigma\partial_\varsigma F_I - \Big[mL_2\sigma^3 + \Big(p\frac{e_z}{L_2} - (-1)^I kL_2\Big)\sigma^1 - i\sigma^2 qe_z\Big]F_I = 0, \tag{30}$$

where $e_z \equiv (d + z - 3)L_2^2\mu$. In addition, in the above equation, we use the same Gamma matrices as Eq. (18) except $\Gamma^\varsigma = -\Gamma^r$. Thus, the conformal dimension of the dual operator $\mathcal{O}_k$ in the IR CFT is $\delta_k = \frac{1}{2} + \nu_I(k)$ with

$$\nu_I(k) = \sqrt{\big(m^2 + \tilde{m}_I^2\big)L_2^2 - q^2e_z^2}, \tag{31}$$

$$\tilde{m}_I = \frac{pe_z}{L_2^2} - (-1)^I k. \tag{32}$$

Obviously, the Lifshitz dynamical critical exponent z and the dipole coupling p modify together the scaling in the infrared. For $\frac{e_z^2}{L_2^2}q^2 > m^2$, there exists a range of momentum

$$k \in \mathcal{J}_I \equiv \Big[(-1)^I\frac{pe_z}{L_2^2} - k_0, (-1)^I\frac{pe_z}{L_2^2} + k_0\Big], \tag{33}$$

where $k_0 \equiv \sqrt{\frac{e_z^2}{L_2^2}q^2 - m^2}$ and $\nu_I(k)$ becomes pure imaginary. We refer to this region of momentum space as the oscillatory region [7,15,16], in which the peaks lose its status as a Fermi surface. The oscillatory regions are different for the dual operator $\mathcal{O}_1$

[2] Here we will only focus on the case of $d = 3$.

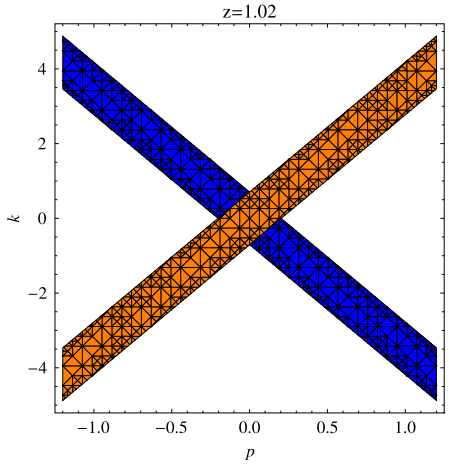

Fig. 1. The oscillatory region for $z = 1.02$ ($q = 0.5$). The orange band denotes $\mathcal{J}_2$ and blue band $\mathcal{J}_1$. (For interpretation of the references to color in this figure legend, the reader is referred to the web version of this article.)

and $\mathcal{O}_2$. Only when $p = 0$, are the oscillatory regions coincident. In Fig. 1, we show the plots of the oscillatory region $\mathcal{J}_I$ vs. p for $z = 1.02$.

In addition, we show the Fermi momentum k_F as a function of p (negative p and small positive p) in Fig. 2 for different Lifshitz dynamical exponent z. The dashed blue line denotes a p_0 and when $p > p_0$, the peaks begin to enter the oscillatory region and lost the meaning as Fermi surfaces. We can easily determine the values of p_0 as follows: $p_0 \simeq 0.11$ for $z = 1.02$, $p_0 \simeq 0.04$ for $z = 1.1$ and $p_0 \simeq -0.01$ for $z = 1.2$. We find that the peaks enter more quickly into the oscillatory region with the increase of p for larger z. Also we have sampled the Fermi momentum k_F for some values of p for various z in Table 1.

Once the Fermi momentum k_F are worked out numerically, the dispersion relation can be determined by the matching method [7]

$$\tilde{\omega}(\tilde{k}) \propto \tilde{k}^{\delta}, \quad \text{with } \delta = \begin{cases} \frac{1}{2\nu_I(k_F)} & \nu_I(k_F) < \frac{1}{2}, \\ 1 & \nu_I(k_F) > \frac{1}{2}. \end{cases} \tag{34}$$

By using the above equation, the scaling exponents δ of the dispersion relation with different z and p for $q = 0.5$ can be calculated

Table 2
The scaling exponents δ with different z and p for $q = 0.5$.

p	-1	-0.8	-0.6	-0.4	-0.2	0	0.1
$z = 1.02$	1	1	1	1	1.2161	2.3047	5.1905
$z = 1.1$	1	1	1	1	1.4642	3.4638	×
$z = 1.2$	1	1	1	1.05437	1.77554	×	×

in term of the Fermi momentum k_F obtained in Table 2. From this table, we can see that for fixed z, the fermionic system undergoes phase transition from Fermi liquid to marginal Fermi liquid ($\nu_I(k_F) = \frac{1}{2}$) and to non-Fermi liquid when tuning the dipole coupling p. For different z, the transition point from Fermi liquid to non-Fermi liquid is different. Obviously, the transition point decreases with the increase of the dynamical Lifshitz critical exponent z.

4. Emergence of the gap

Now we turn to consider the case of the large dipole coupling p. Fig. 3 shows the 3d and density plots of the spectral function $A(\omega, k)$ for $z = 1.02$ and $p = 3$, from which a gap is obviously visible around $\omega = 0$ instead of a sharp peak. In addition, two bands locate at the positive frequency and negative frequency regions, respectively and the strength of the lower band is bigger than the upper band. By showing $A(\omega, k)$ as a function of ω for some fixed values of k for $p = 2.2$ and $z = 1.02$ in the left plot above in Fig. 4, one observes that as $\omega = 0$ is approached, the strength of the peaks degrades and finally vanishes around $\omega = 0$, indicating that a gap opens. The strength of the peak at the negative frequency is bigger than that at the positive frequency, which is consistent with that found in the 3d and density plots in Fig. 3.

To proceed, we would like to focus on the refined characteristic of the gap including the density state $A(\omega)$ and the gap width Δ to test the robustness of the emergence of the gap in this model and see how does the Lifshitz dynamical critical exponent z affect the gap. The density of states $A(\omega)$ is the total spectral weight, which is defined as the integral of the spectral function $A(\omega, k)$. In the right plot above in Fig. 4, the density of states $A(\omega)$ as a function of ω for various p and fixed $z = 1.02$ is showed. From this plot, a relatively high spectral weight around $\omega = 0$ for $p = 0$ is observed. However, as the dipole coupling p

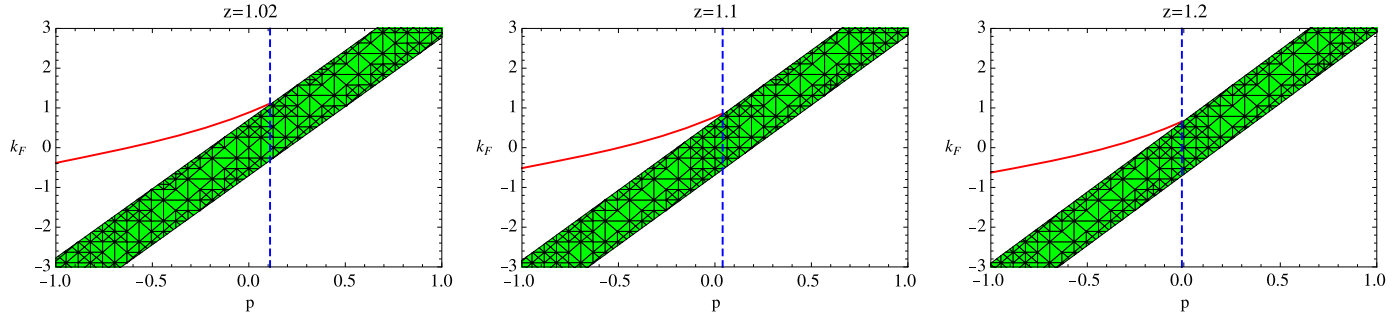

Fig. 2. The Fermi momentum k_F vs. p for various z ($q = 0.5$). The green band depicts the oscillatory region $\mathcal{J}_2$ and the blue dashed vertical line denotes a p_0 and when $p > p_0$, the peaks begin to enter the oscillatory region. (For interpretation of the references to color in this figure legend, the reader is referred to the web version of this article.)

Table 1
The Fermi momentum k_F with different z and p for $q = 0.5$. × denotes the peak has enter the oscillatory region and lose its status as a Fermi surface.

p	-1	-0.8	-0.6	-0.4	-0.2	0	0.1
$z = 1.02$	-0.3833	-0.1877	0.0258	0.2640	0.5403	0.8844	1.0903
$z = 1.1$	-0.5137	-0.3251	-0.1162	0.1220	0.4072	0.7822	×
$z = 1.2$	-0.6262	-0.4453	-0.2415	-0.0036	0.29085	×	×

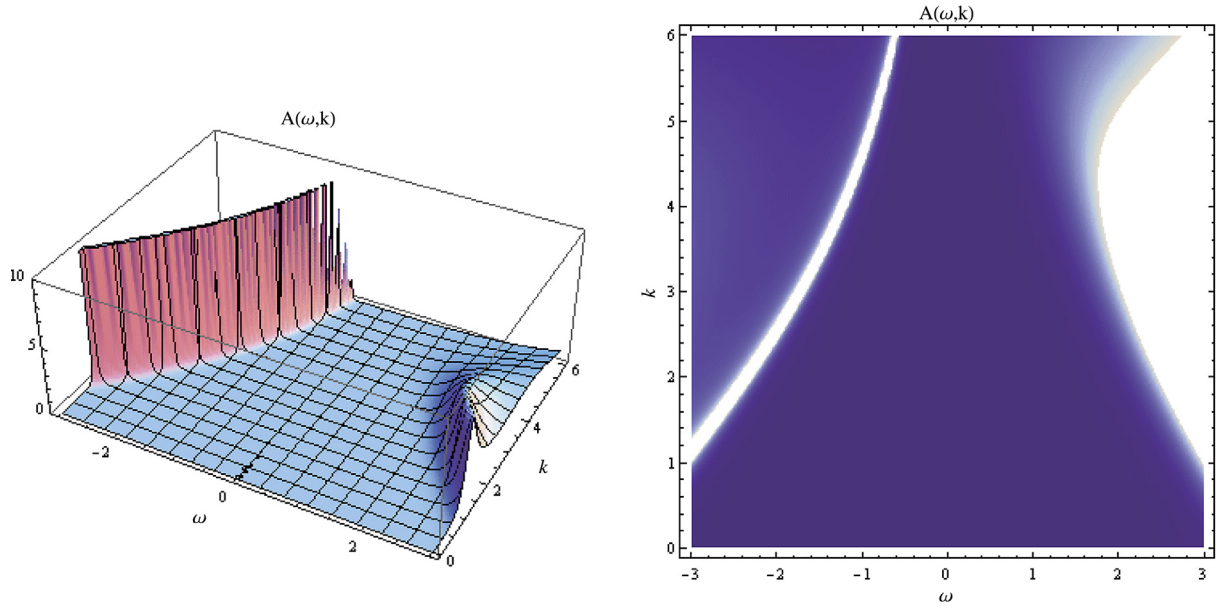

Fig. 3. The 3d and density plots of the spectral function $A(\omega, k)$ for $z = 1.02$ and $p = 3$ ($q = 0.5$ and $m = 0$).

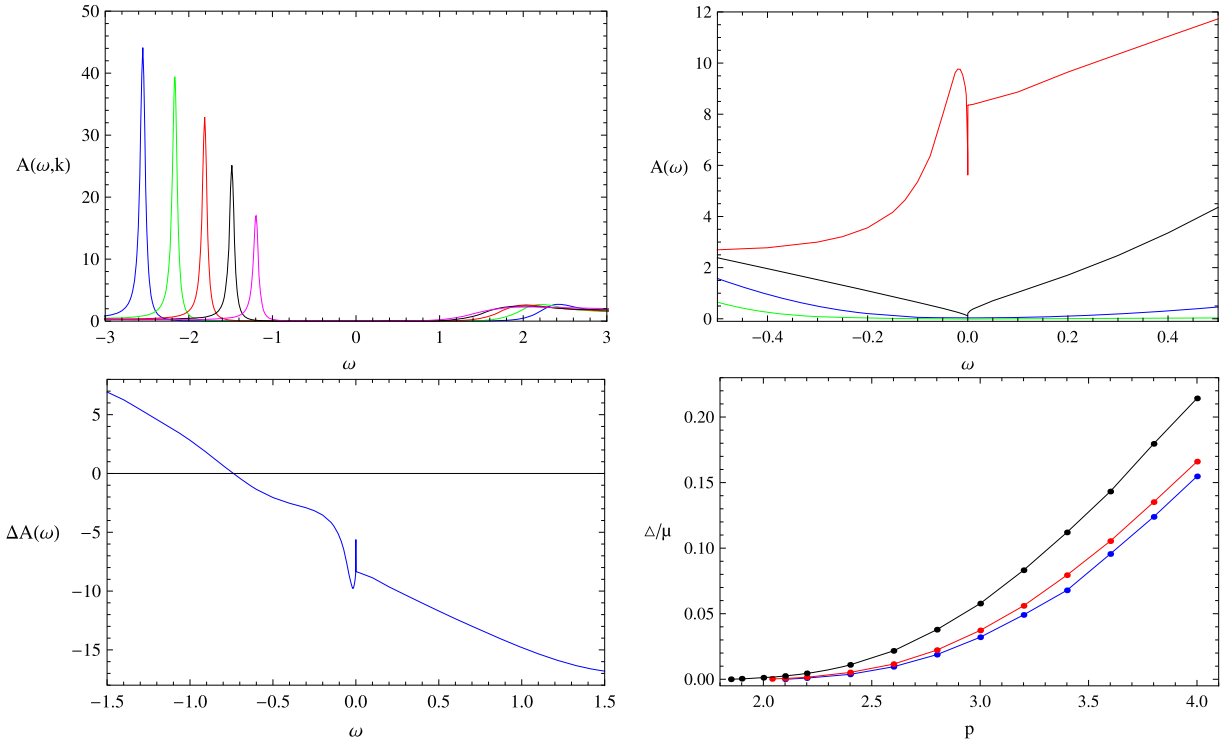

Fig. 4. Left plot above: The spectral function $A(\omega, k)$ vs. ω for sample values of k for $p = 2.2$. Right plot above: The density of state $A(\omega)$ vs. ω for $p = 0$ (red), 1 (black), 2 (blue) and 3 (green). Left plot below: the relation between $\Delta A(\omega) := A(\omega, p = 3) - A(\omega, p = 0)$ and ω. In the two plots above and the left plot below, we take $q = 0.5$, $m = 0$ and $z = 1.02$ as usual. Right plot below: the gap width Δ (in unites of μ) vs. p for various z (blue for $z = 1$, red for $z = 1.02$ and black for $z = 1.1$). Here, we take $q = 0.5$, $m = 0$. (For interpretation of the references to color in this figure legend, the reader is referred to the web version of this article.)

becomes larger, the spectral weight around $\omega = 0$ degrades gradually and vanishes finally. Again, it confirms the existence of the gap for large dipole coupling. On the other hand, the relation between $\Delta A(\omega) := A(\omega, p = 3) - A(\omega, p = 0)$ and ω is also plotted for $z = 1.02$ in the left plot below in Fig. 4 and it indicates there are a transfer of spectral weight over all energy scales. It is similar with the cases found on RN-AdS background or another Lifshitz background from EMP model [15,43].

After having confirmed the robustness of the emergence of the gap in Lifshitz background from EDM model, we will further see how does z affect the gap. First, in term of the density of state $A(\omega)$, we will determine the critical dipole coupling strengths p_c indicating the onset of the gap for various z. By careful numerical computations, we can determine $p_c \simeq 2.1$ for $z = 1$, $p_c \simeq 2.04$ for $z = 1.02$ and $p_c \simeq 1.1$ for $z = 1.1$. It indicates that the onset of the gap becomes easier with the increase of z. To illustrate this point,

we study further the relation of the width of the gap Δ vs. p for various z. From the right plot below Fig. 4, we can see that for the fixed z, the width of the gap Δ increases with the increase of p, which is similar with that found in the another Lifshitz black hole from EMP model [43]. In addition, we also note that for the same p, the width of the gap Δ becomes larger with the increase of z. It indicates that the gap opens easier for the larger z from another point of view.

Before closing this section, we would like to give some comments on the physics that we find in this section. Here we find two key features of the fermionic spectral function with dipole coupling on this Lifshitz background. One is that a gap opens up when the dipole coupling p is beyond a critical value p_c. Another one is that there is a transfer of spectral weight over all energy scales. The two features are also that Mott insulators possess [47–51] and have been also found on the RN-AdS, Gauss–Bonnet AdS and dilaton black branes by AdS/CFT duality [15,16,20,22]. The emergence of the gap on this Lifshitz background further confirms the robustness that dipole coupling can open a gap. The Lifshitz dynamical critical exponent z only plays the role of making the gap open easier.

5. Conclusions and discussion

In this Letter, we have studied the properties of the fermionic spectral function in the presence of a bulk dipole coupling on the charged Lifshitz black hole from EDM model. By analyzing the low energy behaviors of the Dirac equations on the near horizon geometry of this Lifshitz background, we find that the conformal dimension of the dual operator $\mathcal{O}_{\vec{k}}$ in the IR CFT is modified by the Lifshitz dynamical critical exponent z and the dipole coupling p together. Therefore, there are different critical values p_0, which denotes that the peaks begin to enter the oscillatory region, for different z. The peaks enter more quickly into the oscillatory region as p increases for larger z. By studying the dispersion relation for negative and small positive p, we find that for fixed z, the fermionic system undergoes phase transition from Fermi liquid to marginal Fermi liquid and to non-Fermi liquid with the increase of p. For different z, the transition point is different, which decreases as the dynamical Lifshitz critical exponent z increases.

Furthermore, we investigate the large dipole coupling effects on this background. For fixed z, when p goes beyond a critical value p_c, the Fermi sea disappears and a gap opens up as that found in RN-AdS background [15,16]. In addition, there is also a transfer of spectral weight over all energy scales. These two features indicate that the fermionic systems on the charged Lifshitz background can model the Mott insulators. By studying density of states $A(\omega)$ and the width of the gap Δ for different z, we find that the gap opens easier for the larger z.

Comparing with the dipole fermionic response on the another Lifshitz background from EMP model, in which only is a specific Lifshitz dynamical exponent z explored, here we can tune continuously the dynamical exponent z so that we can study how does the exponent z affect the phase transition from Fermi liquid to marginal Fermi liquid to non-Fermi liquid and to Mott gap. Since Lifshitz geometry is a non-relativistic fixed point, it seems to be more natural to impose a Lorentz violating boundary term for a Dirac spinor [44]. Therefore, it is interesting to extend our studies to the non-relativistic fermionic fixed point. In addition, we would also like to mention a recent interesting paper [52], in which the transport coefficients are calculated on the same charged Lifshitz background. They find some novel features of the transport coefficients on this Lifshitz black branes background. Especially, some nontrivial power law behavior in the real part of optical conductivity in the high frequency regime are found. They argue that their results perfectly match with the so-called hopping conductivity which is often found in extreme disordered solids.[3] Therefore, in order to find a deep connection between our results in this or previous paper [42] and that in [52], it will be interesting to calculate the optical conductivity of the fermionic system on this Lifshitz black branes background.

Acknowledgements

This work is partly supported by the NSFC under grant Nos. 11305018 and 11275208.

References

[1] J.M. Maldacena, The large N limit of superconformal field theories and supergravity, Adv. Theor. Math. Phys. 2 (1998) 231, arXiv:hep-th/9711200.
[2] S.S. Gubser, I.R. Klebanov, A.M. Polyakov, Gauge theory correlators from non-critical string theory, Phys. Lett. B 428 (1998) 105–114, arXiv:hep-th/9802109.
[3] E. Witten, Anti-de Sitter space and holography, Adv. Theor. Math. Phys. 2 (1998) 253–291, arXiv:hep-th/9802150.
[4] S.S. Lee, A non-Fermi liquid from a charged black hole: a critical Fermi ball, Phys. Rev. D, Part. Fields 79 (2009) 086006, arXiv:0809.3402.
[5] H. Liu, J. McGreevy, D. Vegh, Non-Fermi liquids from holography, Phys. Rev. D, Part. Fields 83 (2011) 065029, arXiv:0903.2477.
[6] M. Čubrović, J. Zaanen, K. Schalm, String theory, quantum phase transitions and the emergent Fermi-liquid, Science 325 (2009) 439, arXiv:0904.1993.
[7] T. Faulkner, H. Liu, J. McGreevy, D. Vegh, Emergent quantum criticality, Fermi surfaces and AdS_2, Phys. Rev. D, Part. Fields 83 (2011) 125002, arXiv:0907.2694.
[8] J.P. Wu, Holographic fermions in charged Gauss–Bonnet black hole, J. High Energy Phys. 1107 (2011) 106, arXiv:1103.3982.
[9] J.P. Wu, Some properties of the holographic fermions in an extremal charged dilatonic black hole, Phys. Rev. D, Part. Fields 84 (2011) 064008, arXiv:1108.6134.
[10] W.J. Li, J.P. Wu, Holographic fermions in charged dilaton black branes, arXiv:1203.0674.
[11] N. Iizuka, N. Kundu, P. Narayan, S.P. Trivedi, Holographic Fermi and non-Fermi liquids with transitions in dilaton gravity, J. High Energy Phys. 1201 (2012) 094, arXiv:1105.1162.
[12] W.J. Li, H. Zhang, Holographic non-relativistic fermionic fixed point and bulk dipole coupling, J. High Energy Phys. 1111 (2011) 018, arXiv:1110.4559.
[13] W.J. Li, R. Meyer, H. Zhang, Holographic non-relativistic fermionic fixed point by the charged dilatonic black hole, J. High Energy Phys. 1201 (2012) 153, arXiv:1111.3783.
[14] Y. Ling, C. Niu, J.P. Wu, Z. Xian, H. Zhang, Holographic fermionic liquid with lattices, arXiv:1304.2128.
[15] M. Edalati, R.G. Leigh, P.W. Phillips, Dynamically generated Mott gap from holography, Phys. Rev. Lett. 106 (2011) 091602, arXiv:1010.3238.
[16] M. Edalati, R.G. Leigh, K.W. Lo, P.W. Phillips, Dynamical gap and cuprate-like physics from holography, Phys. Rev. D, Part. Fields 83 (2011) 046012, arXiv:1012.3751.
[17] I. Bah, A. Faraggi, J.I. Jottar, R.G. Leigh, L.A. Pando Zayas, Fermions and $D = 11$ supergravity on squashed Sasaki–Einstein manifolds, J. High Energy Phys. 1102 (2011) 068, arXiv:1008.1423.
[18] I. Bah, A. Faraggi, J.I. Jottar, R.G. Leigh, Fermions and type IIB supergravity on squashed Sasaki–Einstein manifolds, J. High Energy Phys. 1101 (2011) 100, arXiv:1009.1615.
[19] D. Guarrera, J. McGreevy, Holographic Fermi surfaces and bulk dipole couplings, arXiv:1102.3908.
[20] J.P. Wu, H.B. Zeng, Dynamic gap from holographic fermions in charged dilaton black branes, J. High Energy Phys. 1204 (2012) 068, arXiv:1201.2485.
[21] W.Y. Wen, S.Y. Wu, Dipole coupling effect of holographic fermion in charged dilatonic gravity, Phys. Lett. B 71 (2) (2012) 266–271, arXiv:1202.6539.
[22] X.M. Kuang, B. Wang, J.P. Wu, Dipole coupling effect of holographic fermion in the background of charged Gauss–Bonnet AdS black hole, J. High Energy Phys. 1207 (2012) 125, arXiv:1205.6674.
[23] X.M. Kuang, B. Wang, J.P. Wu, Dynamical gap from holography in the charged dilaton black hole, arXiv:1210.5735.

[3] We would like to thank S. Y. Wu for pointing out this interesting point in their paper [52].

[24] L.Q. Fang, X.H. Ge, X.M. Kuang, Holographic fermions with running chemical potential and dipole coupling, arXiv:1304.7431.
[25] S. Kachru, X. Liu, M. Mulligan, Gravity duals of Lifshitz-like fixed points, Phys. Rev. D, Part. Fields 78 (2008) 106005, arXiv:0808.1725.
[26] U.H. Danielsson, L. Thorlacius, Black holes in asymptotically Lifshitz spacetime, J. High Energy Phys. 0903 (2009) 070, arXiv:0812.5088.
[27] R.B. Mann, Lifshitz topological black holes, J. High Energy Phys. 0906 (2009) 075, arXiv:0905.1136.
[28] G. Bertoldi, B.A. Burrington, A. Peet, Black Holes in asymptotically Lifshitz spacetimes with arbitrary critical exponent, arXiv:0905.3183.
[29] M. Taylor, Non-relativistic holography, arXiv:0812.0530.
[30] D.W. Pang, A note on black holes in asymptotically Lifshitz spacetime, arXiv:0905.2678.
[31] D.W. Pang, On charged Lifshitz black holes, J. High Energy Phys. 1001 (2010) 116, arXiv:0911.2777.
[32] K. Balasubramanian, J. McGreevy, An analytic Lifshitz black hole, arXiv:0909.0263.
[33] E. Ayon-Beato, A. Garbarz, G. Giribet, M. Hassaine, Lifshitz black hole in three dimensions, Phys. Rev. D, Part. Fields 80 (2009) 104029, arXiv:0909.1347.
[34] R.G. Cai, Y. Liu, Y.W. Sun, A Lifshitz black hole in four dimensional R2 gravity, J. High Energy Phys. 0910 (2009) 080, arXiv:0909.2807.
[35] Y.S. Myung, Y.W. Kim, Y.J. Park, Dilaton gravity approach to three dimensional Lifshitz black hole, Eur. Phys. J. C 70 (2010) 335–340, arXiv:0910.4428.
[36] M.H. Dehghani, R. Pourhasan, R.B. Mann, Charged Lifshitz black holes, Phys. Rev. D, Part. Fields 84 (2011) 046002, arXiv:1102.0578.
[37] V. Keranen, L. Thorlacius, Thermal correlators in holographic models with Lifshitz scaling, Class. Quantum Gravity 29 (2012) 194009, arXiv:1204.0360.
[38] J. Tarrio, S. Vandoren, Black holes and black branes in Lifshitz spacetimes, J. High Energy Phys. 1109 (2011) 017, arXiv:1105.6335.
[39] U. Gursoy, E. Plauschinn, H. Stoof, S. Vandoren, Holography and ARPES sum-rules, J. High Energy Phys. 1205 (2012) 018, arXiv:1112.5074.
[40] M. Alishahiha, M.R.M. Mozaffar, A. Mollabashi, Fermions on Lifshitz background, arXiv:1201.1764.
[41] L.Q. Fang, X.H. Ge, X.M. Kuang, Holographic fermions in charged Lifshitz theory, Phys. Rev. D, Part. Fields 86 (2012) 105037, arXiv:1201.3832.
[42] J.P. Wu, Holographic fermions on a charged Lifshitz background from Einstein–Dilaton–Maxwell model, J. High Energy Phys. 1303 (2013) 083.
[43] J.P. Wu, Emergence of gap from holographic fermions on charged Lifshitz background, J. High Energy Phys. 1304 (2013) 073.
[44] J.N. Laia, D. Tong, A holographic flat band, arXiv:1108.1381.
[45] N. Iqbal, H. Liu, Real-time response in AdS/CFT with application to spinor, Fortschr. Phys. 57 (2009) 367–384, arXiv:0903.2596.
[46] M.R.M. Mozaffar, A. Mollabashi, Holographic quantum critical points in Lifshitz space–time, arXiv:1212.6635.
[47] N.F. Mott, Proc. Phys. Soc. A 62 (1949) 416.
[48] P. Phillips, Mottness: Identifying the propagating charge modes in doped Mott insulators, Rev. Mod. Phys. 82 (2010) 1719, arXiv:1001.5270.
[49] M.B.J. Meinders, H. Eskes, G.A. Sawatzky, Phys. Rev. B 48 (1993) 3916.
[50] C.T. Chen, et al., Phys. Rev. Lett. 66 (1991) 104.
[51] R.G. Leigh, P. Phillips, Origin of the Mott gap, Phys. Rev. B 79 (2009) 245120, arXiv:0812.0593.
[52] J.R. Sun, S.Y. Wu, H.Q. Zhang, Novel features of the transport coefficients in Lifshitz black branes, arXiv:1302.5309.